Journal of Applied Polymer Science

# An *in situ* intercalative polymerization method for preparing UV curable clay–polymer nanocomposites

**Erin Pavlacky, Dean C. Webster**
Department of Coatings and Polymeric Materials, North Dakota State University, PO Box 6050, Dept 2760, Fargo 58108, North Dakota
Correspondence to: D. C. Webster (E-mail: dean.webster@ndsu.edu)

**ABSTRACT:** A novel *in situ* intercalative polymerization technique was used to disperse clay mineral in a precursor resin for use in UV curing by performing an *in situ* ion exchange reaction during polyesterification. Unmodified montmorillonite (MMT) was added to a reaction mixture composed of monomers and methyl, tallow, bis-2-hydroxyethyl ammonium (MTEtOH) during the synthesis of unsaturated polyesters to create resins containing highly dispersed, organically modified MMT. UV-curable clay–polymer nanocomposite (CPN) films were then prepared utilizing donor–acceptor chemistry through reactions of the unsaturated polyester resin with triethylene glycol divinyl ether. Functional group conversion improved up to 15% by the incorporation of clay mineral into the polymer matrix through the *in situ* polymerization method. The CPNs also had improved barrier, mechanical, and thermal properties over a control film containing no clay mineral. © 2015 Wiley Periodicals, Inc. J. Appl. Polym. Sci. **2015**, *132*, 42601.

**KEYWORDS:** clay; coatings; composites; photopolymerization

Received 31 December 2014; accepted 10 June 2015
**DOI: 10.1002/app.42601**

## INTRODUCTION

The incorporation of nanosized clay minerals into polymer matrices has resulted in clay–polymer nanocomposites (CPNs) exhibiting significant improvements in material properties including thermal stability,[1–4] tensile strength,[5–8] barrier protection,[9–12] and flame retardancy.[13,14] CPNs have emerged as viable alternatives to conventional microcomposite systems, where much lower filler concentrations (1–5 mass %) are utilized compared to the traditional phase-separated composites (20–30 mass %).[15–18] Montmorillonites, a member of the 2 : 1 phyllosilicate family, are commonly employed in the production of CPNs due to their ease of intercalation which can be used to organically modify the inorganic surface along with low cost as a result of their natural abundance in nature.[19] The montmorillonite (MMT) structure consists of one alumina octahedral sheet embedded between two silica tetrahedral sheets; isomorphic substitutions of trivalent aluminum within the clay layers lead to negatively charged MMT platelets. To counterbalance the excess negative charge, cations, such as $Na^+$, are located between each MMT layer. Strong polymer/clay mineral interactions are important to the final dispersion of layered silicates within polymer matrices and organic modification of hydrophilic clay mineral surfaces is used to increase the organophilicity of the inorganic fillers.[20] Commonly, quaternary ammonium cationic surfactants are used to lower the surface energy and help render the clay mineral organophilic.[21]

Polymer/clay mineral composite morphology is typically categorized as phase-separated, intercalated, or exfoliated. Phase-separated morphology describes flocculation of clay mineral layers from interactions between the hydroxylated clay mineral edges, differences in polymer and clay mineral surface tensions, and immiscibility leading to microcomposite morphologies.[20,22,23] Intercalated CPN morphologies consist of regularly stacked clay mineral platelets with polymer penetrating into the clay mineral interlayer, whereas exfoliated morphologies describe the homogenous dispersion of delaminated individual clay mineral platelets throughout the polymer matrix.[24] Three main intercalative techniques have been developed to successfully disperse the layered silicates in the host polymer: melt intercalation, polymer intercalation from solution, and *in situ* intercalative polymerization. The melt intercalation technique consists of annealing molten polymer and clay mineral to swell the silicate layers with polymer, when there is sufficient miscibility, to form intercalated or exfoliated morphologies. *In situ* intercalative polymerizations consist of initially swelling the clay mineral in a monomer or monomer solution followed by inducing the polymerization within and surrounding the silicate layers, creating a highly dispersed CPN. Of these techniques, *in situ* intercalative polymerization may be the most advantageous as the technique is highly efficient, theoretically solvent-free, and combines the polymerization and intercalation steps into a single, simultaneous process.[25]

*In situ* polymerization to intercalate or exfoliate layered silicates has been studied in a variety of polymers with various organic modifications. Messersmith and Giannelis studied the initiation and propagation mechanisms during the intercalation of layered silicates through *in situ* intercalative polymerization of ε-caprolactone.[26] Paul *et al.* utilized organic modifiers bearing hydroxy groups to graft poly(L,L-lactide) to the modified clays to create exfoliated CPNs via ring-opening *in situ* intercalative polymerization.[27] Similar *in situ* intercalative polymerization utilizing hydroxy-functional organic modifiers have been reported in the production of CPN systems including polyethers,[28] polyurethanes,[29,30] phenolic resins,[31] and acrylic resins.[32]

Previously, the development of UV-curable polyester CPN films through a novel *in situ* preparation technique was reported.[33] Liquid monomer diethylene glycol and Cloisite® 30B, a commercially available hydroxy-functional MMT, were dispersed at high shear, followed by synthesis of unsaturated polyester resins containing 1–10 mass % clay mineral. UV-curable CPN films were formed utilizing donor–acceptor chemistry to produce intercalated and exfoliated films with increased conversion, water vapor barrier protection, and mechanical performance.

Based on the success of obtaining high clay mineral dispersion using the *in situ* polymerization technique, the present study explores a novel *in situ* technique to further increase clay mineral dispersion. Typically, *in situ* intercalative polymerizations involve creating a precursor dispersion of organomodified clay mineral and monomer, followed by polymerization to induce delamination of the clay mineral platelets by the increased volume of the polymer chains between clay mineral platelets. In contrast, this novel *in situ* polymerization technique is characterized by the addition of unmodified MMT *during* polyesterification to a reaction mixture already containing MTEtOH, a hydroxy-functional alkylammonium organic modifier. Through this process, the unmodified clay mineral may undergo an *in situ* ion exchange reaction with the alkylammonium surfactant, and be dispersed uniformly throughout the polyester resin. Thus, a unique feature of this novel *in situ* intercalative polymerization is the simultaneous polyesterification and ion exchange reaction between the MTEtOH organic modifier and unmodified MMT clay. This new *in situ* technique was compared to a clay mineral dispersion technique of mixing and sonication to study the impact of the dispersion route.

## EXPERIMENTAL

### Materials

Monomers 1,6-hexanediol, maleic anhydride, and diethylene glycol were obtained from Sigma Aldrich (Milwaukee, WI) along with reactive diluent tri(ethylene glycol) divinyl ether (TEGDVE) and iodomethane. Monomer 1,4-cyclohexanedicarboxylic acid (1,4-CHDA) was obtained from Eastman Chemical Company (Kingsport, TN). The photoinitiator Darocur® 1173, 2-hydroxy-2-methyl-1-phenyl-propan-1-one, was obtained from CIBA (Basel, Germany). Ethomeen T/12, a bis(2-hydroxyethyl) tallow alkyl amine, was generously supplied from AkzoNobel (Houston, TX). Cloisite $Na^+$, a naturally occurring montmorillonite clay mineral, was obtained from Southern Clay Products (Gonzales, TX). All reagents were used as received without further purification.

### Preparation of Organic Modifiers

The procedure for the preparation of MTEtOH, the organic modifier of Cloisite® 30B, has been reported earlier.[34] Briefly, Ethomeen T/12 (10.00 g) was quaternized with iodomethane (11.95 g) in dimethylsulfoxide at 23°C, precipitated, and dried in a vacuum oven at room temperature.

### *In Situ* Polymerization

The unsaturated polyester resins were synthesized using a standard melt polyesterification process. First, liquid monomer diethylene glycol and MTEtOH were homogenized at high shear, and then mixed overnight via magnetic stir bar. The monomer/organic modifier solution was weighed with the remaining monomers and added to a 250 mL three-neck RBF equipped with a temperature probe/controller, mechanical stirrer, nitrogen inlet, condenser, heating mantle, and water collection flask according to a previous study.[33] The monomer composition was constant for each polyesterification: maleic anhydride (1.000 mol), diethylene glycol (0.824 mol), 1,6-hexanediol (0.625 mol), and 1,4-CHDA (0.172 mol). The reaction mixture was carefully ramped to 60, 120, and 180°C under an $N_2$ atmosphere. When the reaction mixture stabilized at the intermediate temperature, 120°C, Cloisite® $Na^+$ was added to the reaction flask. The polyester polymerization continued until an acid number of approximately 20 mg KOH/g of resin was achieved. The MTEtOH and Cloisite® $Na^+$ masses were based on the Cloisite® 30B organic modifier content (30 mass %), and the desired clay mineral loading in the final CPN (1, 2, 5, and 10 mass %). For example, 1 mass % Cloisite® 30B with this *in situ* process would be 1.20 g (based on ≈120 g of monomer). Therefore, 0.36 g of MTEtOH and 0.84 g of Cloisite® $Na^+$ was used to achieve an organically modified clay mineral loading similar to the loading of Cloisite® 30B clay.

### Sonication Dispersion Technique

With the sonication dispersion route, unsaturated polyesters were synthesized as described above, but the Cloisite® $Na^+$ was added to the MTEtOH-containing polyester resin after polymerization, mixed to uniformity, and sonicated for 8 h with an ultrasonic bath. Again, the clay mineral loading for this technique was 1, 2, 5, and 10 mass %.

### Coating Preparation

CPN coatings were formulated based on a 1 : 1 stoichiometric ratio between the maleate and vinyl ether functional groups from the unsaturated polyester and TEGDVE, respectively. Photoinitator Darocur® 1173 was added to the unsaturated polyester and reactive diluent mixture based on 6 mass % of the polyester, diluent, and clay mineral. The formulation was mixed to uniformity with a hand spatula, left undisturbed for 1–2 h for air bubble dissipation, and then deposited onto glass and aluminum substrates with a Gardco bar-coater with five mil wet clearance (final film thickness ≈85 μm). The coated substrates were subjected to UV irradiation (Dymax 200 EC silver lamp, UV-A, 365 nm, intensity ≈40 mW/cm$^2$) until the CPN coatings were tack-free (approximately 60 s). The films were allowed to equilibrate for 24 h at room temperature before evaluation.

### Nomenclature

The unsaturated polyesters are named based on the mass % organically modified clay mineral and the clay mineral dispersion technique. The polyester name is as follows: mass % MTEtOH-modified dispersion method. For example, R1_insitu denotes the polyester containing 1 mass % MTEtOH-modified clay mineral prepared through the *in situ* technique. The prefix "R" is used to distinguish the *in situ* or sonication clay mineral dispersion route was utilized in this study. The coatings were named similarly, but have a "NC" prefix to specify the CPN derived from a particular polyester.

### Characterization

The polyester resin molecular weight, viscosity, and glass transition temperature ($T_g$) were characterized prior to film formation. Molecular weight was determined using a Waters 2410 Gel Permeation Chromatograph equipped with a refractive index detector. A 1% sample solution was created by dissolving the polymer sample in solvent tetrahydrofuran (THF). The flow rate was 1 mL/min, and calibration was performed with polystyrene standards. The polyester viscosity was determined using an ICI cone and plate viscometer at 100°C. Differential scanning calorimetry was employed to measure the polyester $T_g$ using a TA Instruments Q1000 Series DSC. The heat–cool–heat test method was applied, where polyester samples were first equilibrated at −90°C, heated to 100°C at a rate of 10°C/min, cooled to −90°C at a rate of 10°C/min, then heated once again to 100°C at a rate of 10°C/min. The polyester $T_g$ was determined from the inflection point in the second heating cycle.

Real-time infrared spectroscopy (RTIR) measurements were performed using a Thermo Nicolet Magna-IR 850 spectrometer with detector type DTGS KBr. The UV irradiation source for curing the samples was a LESCO Super Spot MK II UV-curing lamp equipped with a fiber-optic light guide. Each formulation was spin-coated onto a KBr window at 3000 RPM, placed in the spectrometer chamber, and was simultaneously exposed to UV and infrared irradiation. The coated KBr windows were approximately 20 mm from the fiber-optical cable (light intensity ≈10 mW/cm$^2$). The degree of conversion was determined from the disappearance of the vinyl ether double bonds (1639 cm$^{-1}$) and calculated from

$$\%\ conversion = \left\{ \left[ (A_{1639})_0 - (A_{1639})_t \right] / (A_{1639})_0 \right\} \times 100$$

where $(A_{1639})_0$ is the absorbance at time = 0 and $(A_{1639})_t$ is the absorbance at time *t*.

X-ray powder diffraction was collected using a Bruker AXS' D8 Discover diffractometer in Bragg–Brentano geometry, using Cu Kα radiation with a wavelength of 1.5406 Å. Samples for TEM were thin cut using a diamond knife and RMC MTXL ultramicrotome. The thin sections were placed on 400 mesh copper grids and photographed using a JEOL 100 cx-II transmission electron microscope operating at 80kV. ASTM E96, "Standard Test Methods for Water Vapor Transmission, Water Method," was employed for characterizing the barrier performance of the CPN films. Samples were placed inside a controlled humidity chamber with conditions of 70% ± 2% relative humidity and 20°C ± 2°C. Under steady-state conditions, the mass loss over time correlated with water vapor transmission (WVT) and water vapor permeance (WVP) under steady-state conditions, and duplicate samples were tested to verify these results. Dynamic mechanical analysis (DMA) was done using a TA Instruments Q800 DMA in tensile mode. CPN-free films, approximately 15 mm in length, 5 mm in width, and 0.070–0.080 mm in thickness, were measured using 1 Hz frequency, constant strain of 0.05%, and a heating rate of 5°C/min over a temperature range of −50 to 200°C. Cross-link density was estimated using the theory of rubber elasticity from the storage modulus in the rubbery plateau.[35] Thermogravimetric analysis was done using a TA Instruments Q500. CPN samples were heated in a nitrogen atmosphere from ambient temperatures to 600°C at a rate of 20°C/min. The optical clarity of each cured film was measured by a Varian Cary 5000 UV–vis spectrometer by determining transmittance at 400 nm.

## RESULTS AND DISCUSSION

### *In Situ* Polymerization Technique

In previous studies, an *in-situ* intercalative polymerization was employed to generate highly dispersed hydroxy-functional Mt CPNs in a precursor polyester resin.[33] Exfoliated CPN films were produced at low levels of clay mineral loading (1–2 mass %). The *in situ* process was modified in this study to produce a novel *in situ* polymerization technique to explore the ability to further induce clay mineral exfoliation in a precursor resin. Scheme 1 illustrates the steps involved to induce clay mineral dispersion during polyesterification. The first step is to create a homogenous mixture of MTEtOH and diethylene glycol. Once the homogenous mixture is achieved, the additional monomers (maleic anhydride, 1,6-hexanediol, and 1,4-CHDA) are added to the diethylene glycol/MTEtOH dispersion. The unmodified clay mineral (Cloisite® $Na^+$) is added to the reaction mixture during polyesterification once the temperature is ramped to 120°C. The temperature for the unmodified clay mineral addition was chosen to be in excess of 100°C to ensure the reaction mixture had low viscosity to aid in the dispersion of the unmodified clays. The goal of this method is to perform an *in situ* ion exchange reaction to attach the organic modifier MTEtOH to the unmodified clay mineral. If the MTEtOH organic modifier achieves a high degree of dispersion within the reaction medium, then the unmodified clay mineral may also be highly dispersed in the final polyester resin. In addition, the hydroxy-functionality of the MTEtOH organic modifier will also help in the exfoliation of clay mineral throughout the polyester resin by reacting with acid functional monomers. If the MTEtOH reaction occurs after the *in situ* ion exchange with the unmodified clay, the growing volume of the polyester oligomers may also increase the distance between clay mineral layers. The final polyester resin containing MTEtOH-modified clay mineral may then serve as a precursor system to creating CPN films with exfoliated morphologies.

### Unsaturated Polyester Properties

The polyester resins were fully characterized prior to coating formation as their physical properties may have an impact on many of the CPN film properties. A summary of the

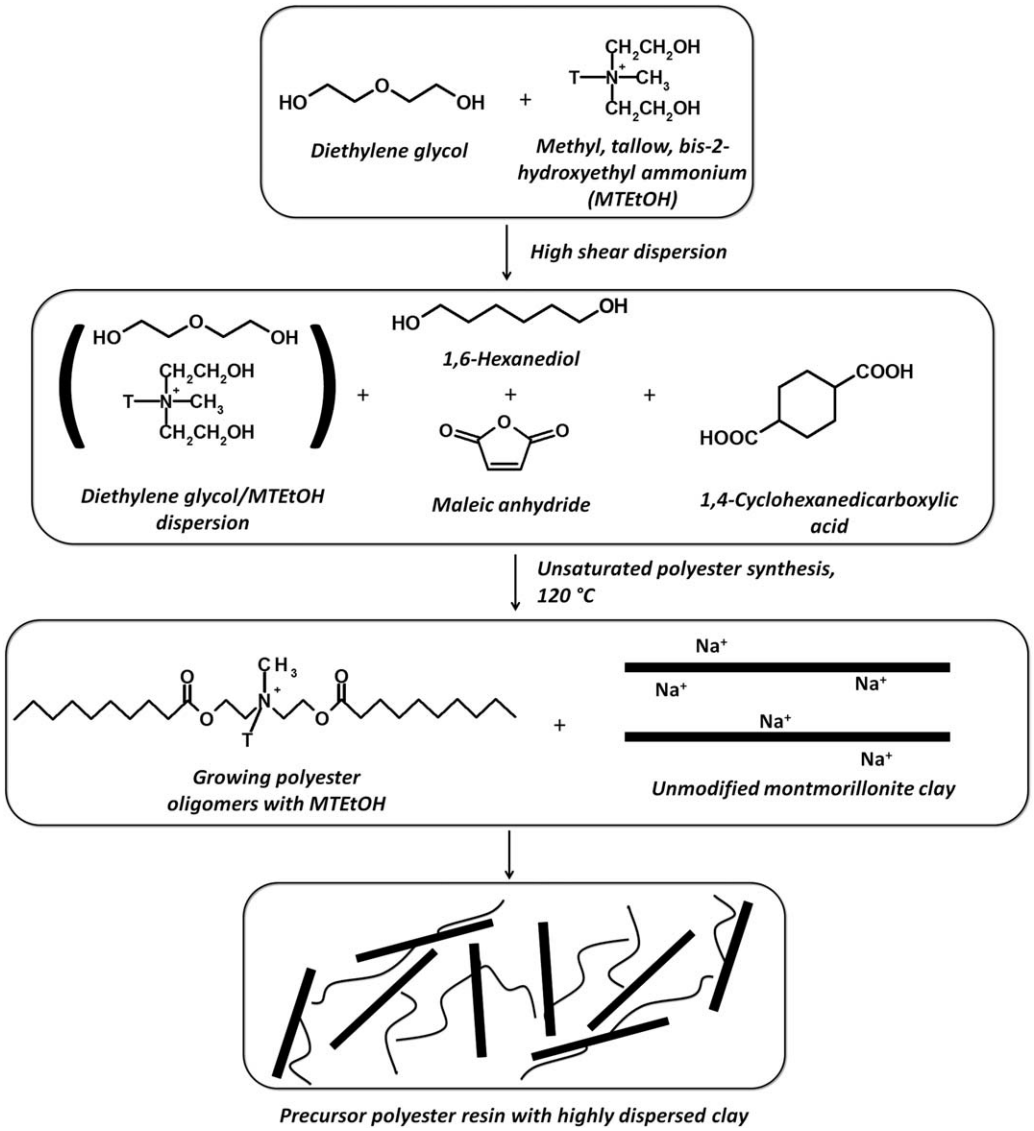


**Scheme 1.** *In situ* polymerization technique to produce highly dispersed, functionalized clay mineral within a polyester resin by undergoing an *in situ* ion exchange reaction.

unsaturated polyester properties are located in Table I. The target acid value was approximately 20 mg KOH/g of polyester; careful monitoring of the acid values of each polyester resin was important to maintain equivalent degrees of polymerization.[36] Consistent acid number values were obtained for each polyester synthesis between 19 and 21 mg KOH/g of polyester.

**Table I.** Unsaturated Polyester Properties

| Polyester name | Acid number | $M_n$ (g/mol) | $M_w$ (g/mol) | PDI | Viscosity (poise) | $T_g$ (°C) |
|---|---|---|---|---|---|---|
| Control | 21 | 1100 | 2400 | 1.9 | 2.4 | −42 |
| R1_insitu | 19 | 1400 | 2900 | 2.1 | 3.2 | −35 |
| R2_insitu | 21 | 1600 | 3200 | 2.0 | 3.4 | −37 |
| R5_insitu | 22 | 1700 | 4100 | 2.4 | 7.2 | −32 |
| R10_insitu | 21 | 1600 | 4100 | 2.6 | 8.8 | −34 |
| R1_sonic | 21 | 1600 | 2900 | 1.8 | 2.6 | −42 |
| R2_sonic | 22 | 1700 | 3100 | 1.9 | 3.2 | −41 |
| R5_sonic | 21 | 1600 | 3000 | 1.9 | 4.0 | −38 |
| R10_sonic | 21 | 1700 | 3400 | 2.0 | 5.4 | −37 |

**Table II.** Cure, Mechanical, Thermal, and Optical Clarity Characterization Data

| Sample name | Conversion | *d*-spacing (nm) | *E′* (MPa, 25°C) | Cross-link density (mol/cm$^3$) | $T_{10}$% (°C) | Transmittance (%) |
|---|---|---|---|---|---|---|
| Control | 72% | — | 370 | 0.022 | 240 | 98 |
| NCR1_insitu | 82% | — | 425 | 0.015 | 300 | 99 |
| NCR2_insitu | 87% | — | 460 | 0.023 | 300 | 93 |
| NCR5_insitu | 82% | 1.50 | 510 | 0.019 | 290 | 91 |
| NCR10_insitu | 78% | 1.69 | 270 | 0.016 | 270 | 70 |
| NCR1_sonic | 74% | — | 535 | 0.037 | 300 | 96 |
| NCR2_sonic | 80% | — | 525 | 0.032 | 290 | 92 |
| NCR5_sonic | 82% | 1.62 | 515 | 0.025 | 285 | 82 |
| NCR10_sonic | 82% | 1.68 | 420 | 0.016 | 290 | 60 |

Incorporation of the MTEtOH modifier and clay mineral into the polyester matrix led to increased molecular weight and PDI values for both clay mineral dispersion routes. As determined by GPC, the $M_n$ for each polyester resin was slightly increased from the control sample, approximately 1600 g/mol, regardless of clay mineral loading or dispersion technique. More dramatic increases in the $M_w$ and PDI were observed, particularly with higher levels of clay mineral loading (5–10 mass %). Polyesters R5_insitu and R10_insitu each had $M_w$ of 4100 g/mol, almost twice the value of the control polyester (2400 g/mol). The polyesters prepared through the sonication dispersion technique had $M_w$ values ranging from 2900 to 3400 g/mol. The mass % clay mineral appeared to have a direct correlation to the $M_w$, where higher clay mineral loading increased $M_w$. The higher molecular weights may be attributed to the greater hydrodynamic volume of the polyester resins containing clay mineral due to interactions between the quaternary ammonium groups with the clay surfaces.

Clay mineral incorporation had a profound impact on the rheological properties of the polyester resins: higher clay mineral content produced significantly higher viscosity systems. Low levels of clay mineral loading (1–2 mass %) increased the polyester viscosity slightly, whereas the higher levels of clay mineral content (5–10 mass %) produced much more viscous resins. The rheological properties of each polyester resin were directly affected by not only the clay mineral content but also the dispersion route. The *in situ* technique generated higher viscosity polyesters than the sonication clay mineral dispersion route for equivalent clay mineral content; the degree of dispersion of clay mineral within the polyester may be a contributing factor to the final resin viscosity.

The *in situ* synthesis technique created polyester resins with higher $T_g$ values than the sonication dispersion route. Each polyester prepared by the *in situ* technique had $T_g$ values 5–10°C higher than the control polyester (−42°C). The increased $T_g$ may be a reflection of decreased mobility of polyester chains due to confinement from the clay mineral platelets. As more clay mineral filler is incorporated into the matrix, the mobility decreases further, resulting in the polyesters with higher clay mineral content having the highest $T_g$ values. Although the same trend is observed with the sonication dispersion route, the $T_g$ increases were not as significant. The $T_g$ value of polyester R10_sonic (−37°C) was 5°C higher than the control resin, which was the most dramatic increase observed with the sonication dispersion route. When comparing $T_g$ values of polyesters with equivalent clay mineral loading, the *in situ* process led to consistently higher $T_g$ values. The final clay mineral dispersion within the polyester resin may be causing the differences in $T_g$ values, where a higher degree of clay mineral dispersion may be impacting the polyester chain mobility to a greater extent through the *in situ* process.

### Cure Characteristics

Donor–acceptor chemistry was employed to create UV-curable CPN coatings derived from the unsaturated polyester resins and reactive diluent TEGDVE. Large increases in the final conversion of the UV-curable coatings compared to the control were observed by monitoring the disappearance of the reactive diluent vinyl ether double bonds at 1639 cm$^{-1}$ (Table II) to determine the extent of the maleate-vinyl ether reaction. With only one exception, the clay mineral-containing formulations,

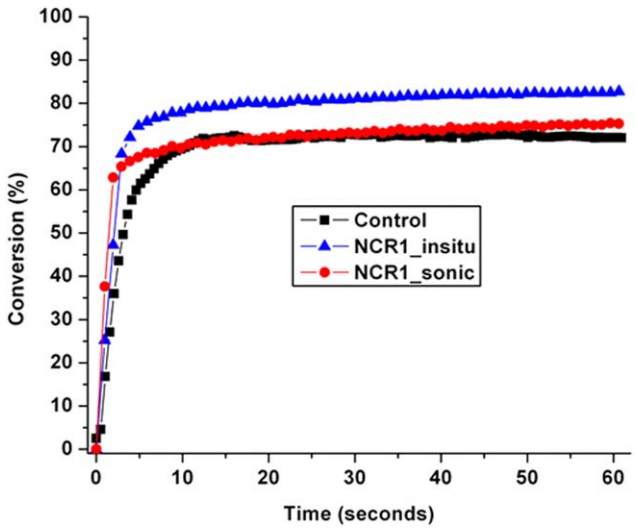


**Figure 1.** Conversion of control, NCR1_insitu, and NCR1_sonic coatings systems determined by disappearance of vinyl ether double bond (1639 cm$^{-1}$) using RTIR (real-time infrared) spectroscopy with 60 s of UV irradiation. [Color figure can be viewed in the online issue, which is available at wileyonlinelibrary.com.]

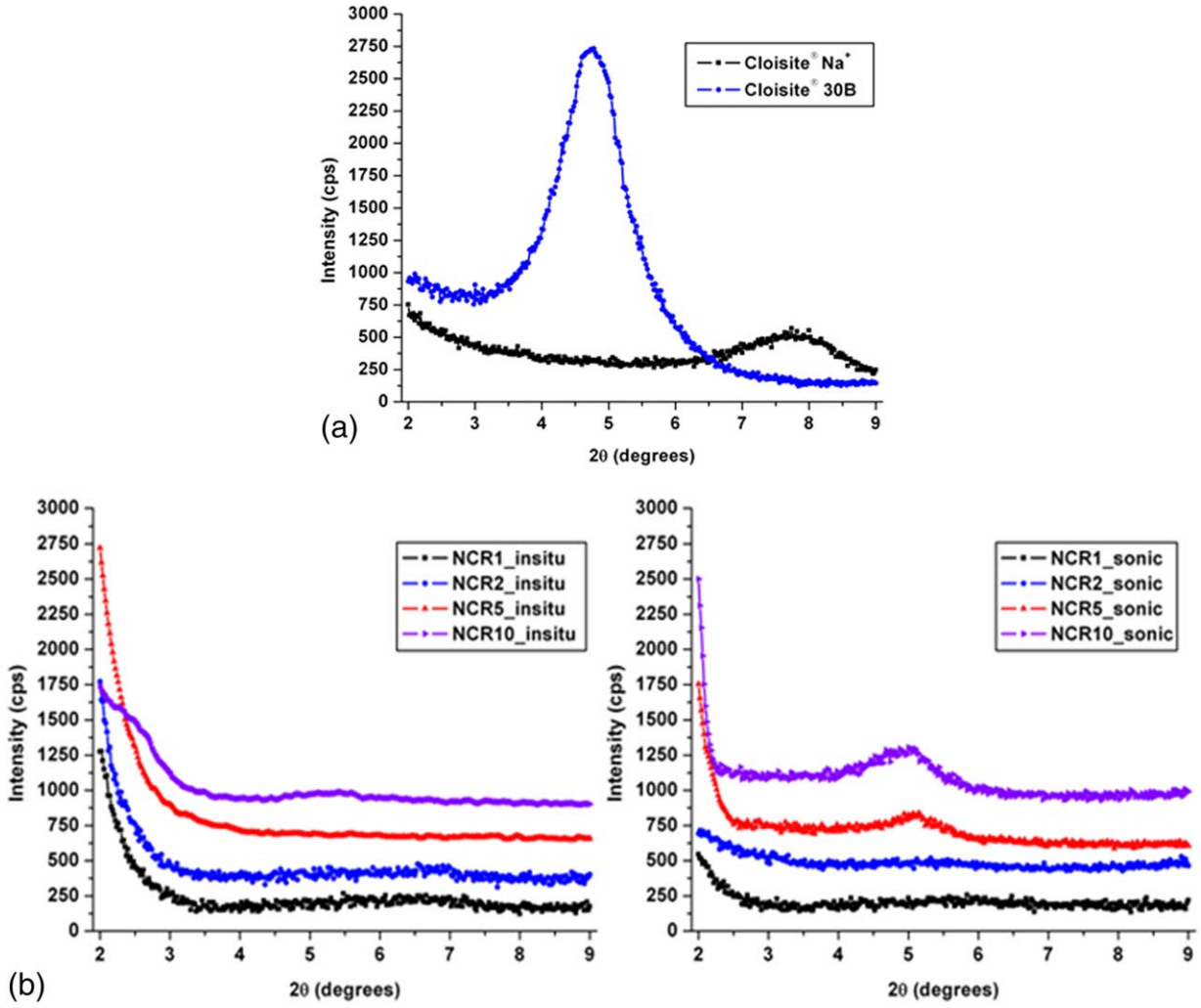


**Figure 2.** XRD scans of (a) the pristine Cloisite® Na+ and Cloisite® 30B and (b) the clay–polymer nanocomposites prepared by the *in situ* and sonication dispersion techniques. [Color figure can be viewed in the online issue, which is available at wileyonlinelibrary.com.]

regardless of dispersion technique, had conversions up to 15% higher than the control formulation containing no clay mineral (72% final conversion). The *in situ* preparation technique produced coatings with higher conversions ranging from 78 to 87%, where, by comparison, the sonication dispersion route coatings had slightly reduced conversions of 74–82%. Figure 1 demonstrates the dramatic conversion increase with the incorporation of just 1 mass % clay mineral. The highest conversion was the coating formulation containing polyester R2_insitu with a conversion of 87%. Increased conversions of the clay mineral-containing formulations may directly correlate to the polyester viscosities. With coating formulation, viscosity increases from the high-viscosity polyesters, reactive chain ends have more difficulty diffusing through the coatings system, thereby decreasing the rate of termination. If the lower molecular weight reactive diluent can still freely diffuse through the coatings system, the final conversion increases from an autoacceleration effect. The same trend was observed in the previous CPN study, where increased viscosity from the clay-containing polyesters produced conversions 10–15% higher than the control formulation.[33]

### CPN Morphology

Clay mineral dispersion within CPNs is typically characterized by two techniques: XRD and TEM. XRD may indicate the degree of clay mineral dispersion based on diffraction peaks occurring between 2 and 9 2$\theta$. From the maximum value of the diffraction peaks in this range, the *d*-spacing, or interlayer distance between clay mineral platelets, can be calculated from Bragg's Law. Figure 2 displays the XRD scans for the pristine clays and CPN films, and *d*-spacing values are reported in Table II. The *d*-spacing of pristine Cloisite® 30B and Cloisite® $Na^+$ were determined to be 1.84 and 1.09 nm, respectively. While the two pristine clay minerals had sharp, prominent diffraction peaks, the CPN samples had significantly lower intensities when the diffraction peaks were resolved. CPNs containing lower levels of clay mineral loading (1–2 mass %) did not indicate any diffraction peaks in the 2–9 2$\theta$ degree range, an indicator of high clay mineral dispersion with random orientation. Conversely, the CPNs containing 5–10 mass % clay mineral had small, wide diffraction peaks. CPNs NCR5_insitu and NCR10_insitu had *d*-spacing values of 1.50 and 1.69 nm, respectively. As these *d*-spacing values were greater than the

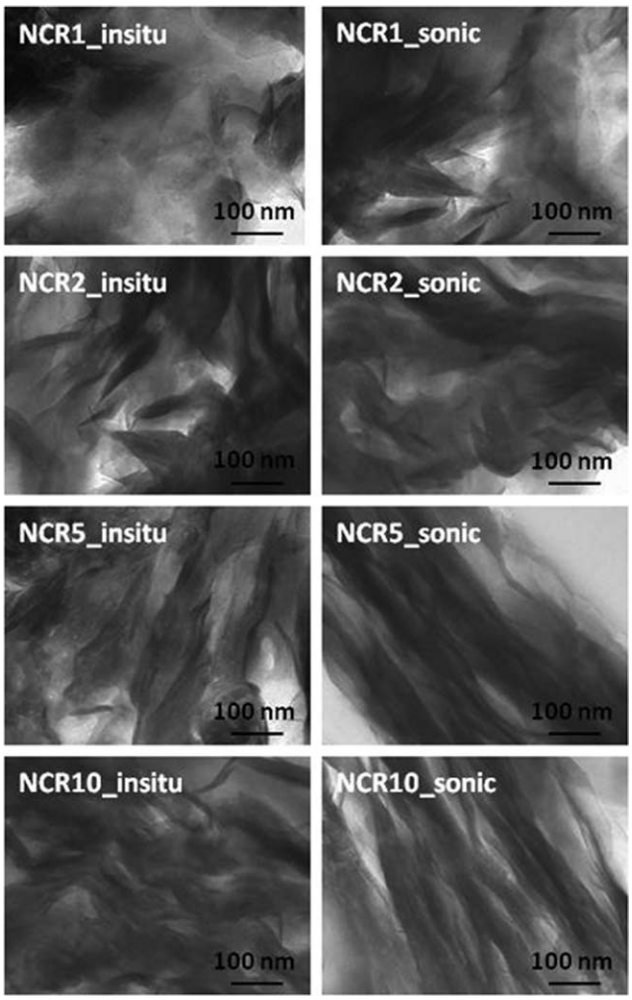


**Figure 3.** TEM micrographs of the UV-cured clay–polymer nanocomposite films.

pristine Cloisite® $Na^+$, the formation of CPNs with intercalated morphologies is indicated. Similarly, the *d*-spacing of CPNs NCR5_sonic (1.62 nm) and NCR10_sonic (1.68 nm) suggest polymer intercalation between clay mineral platelets with overall order maintained. Based on XRD analysis, the level of clay mineral loading had a significant impact on the final degree of clay mineral dispersion, where higher levels of clay mineral filler did not achieve the same extent of dispersion as the CPNs containing 1–2 mass % clay mineral. Although XRD can be an initial indicator of CPN morphology, proper morphological classification must be done in conjunction with TEM.[37] Figure 3 displays the TEM micrographs for the CPNs prepared by both the *in situ* and sonication techniques. The dark lines in the micrographs are cross-sections of the layered silicates dispersed throughout the polyester matrix. From the TEM analysis, it appears that mixed morphologies consisting of exfoliation and intercalation were produced for all *in situ* systems; however, for CPNs with 1 mass % clay, there is a large amount of exfoliation observed the amount of which decreases as the clay loading is increased. CPNs prepared through the mixing and sonication dispersion route appear to be primarily intercalated with portions of phase separation, except for NCR1_sonic, which is classified as partially exfoliated and intercalated.

### Water Vapor Transmission

CPN formation led to reductions in WVT and WVP compared to the control coating. Figures 4 and 5 display the trends in WVT and WVP with increased clay mineral loading, and WVT and WVP data results are reported in Table III. While each CPN film decreased both WVT and WVP, the clay mineral dispersion technique applied in the preparation of each CPN as well as the final clay mineral volume fraction greatly dictated the barrier properties. Two striking trends appeared in the analysis of the CPN barrier results. First, the *in situ* technique produced better barrier films compared to the mixing and sonication clay mineral dispersion route. With the incorporation of just 1 mass % clay mineral, the WVP of NCR1_inistu (9.18E-11 g·m/m$^2$·s·Pa) was one magnitude lower in permeability than the control film (8.79E-10 g·m/m$^2$·s·Pa). Further increases in the clay mineral loading produced lower WVP readings, where NCR5_insitu recorded the lowest WVP (2.96E-11 g·m/m$^2$·s·Pa) for the coatings prepared through the *in situ* process. Although NCR10_inistu had the highest clay mineral volume fraction throughout the polymer matrix, the WVP increased slightly compared to NCR5_insitu (6.70E-11 g·m/m$^2$·s·Pa). The dramatic reductions in the CPN WVT and WVP may be attributed to the dispersion of the nanoscale clay mineral fillers throughout the polymer film, where a highly tortuous diffusion path may form from the incorporation of the impermeable clay mineral platelets.

The uniformity of the clay mineral dispersion also relates to the barrier performance of the CPN films. The second striking trend observed in the barrier properties is the mixing and sonication dispersion technique produced CPNs with increasing WVT and WVP as a function of increased clay mineral loading, an opposite trend than the *in situ* preparation method. NCR1_sonic measured the lowest WVP (1.03E-11 g·m/m$^2$·s·Pa) of the four CPNs prepared through the mixing and sonication technique. Although

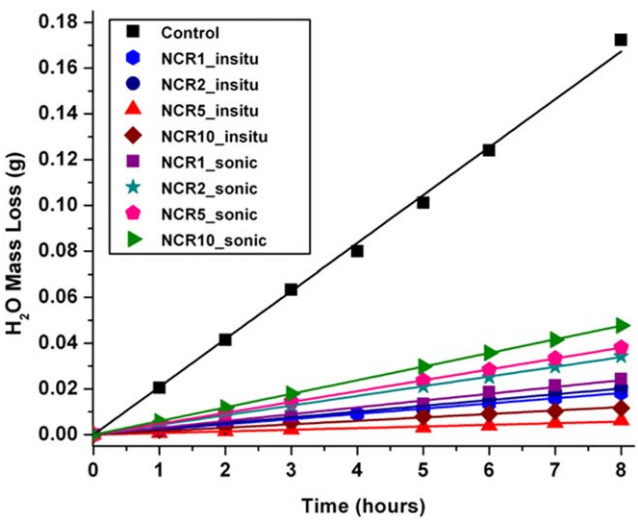


**Figure 4.** Water vapor transmission (WVT) according to ASTM E96 of clay–polymer nanocomposite films. [Color figure can be viewed in the online issue, which is available at wileyonlinelibrary.com.]

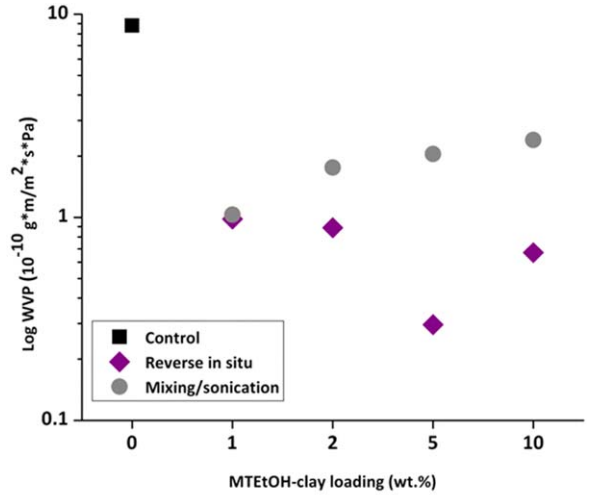


**Figure 5.** Water vapor permeability (WVP) according to ASTM E96 of clay–polymer nanocomposite films. [Color figure can be viewed in the online issue, which is available at wileyonlinelibrary.com.]

the remaining CPNs of the sonication dispersion route measured WVT and WVP lower than the control coating, the barrier properties diminished when the clay mineral loading was increased from 2 to 10 mass % clay mineral. Based on the TEM micrographs and XRD analysis, the dispersion of clay mineral within the cured film may be contributing to the increases in both WVT and WVP. While the incorporation of clay mineral typically improves the barrier properties of polymeric materials by introducing a tortuous diffusion path, high uniformity of the clay mineral distributed throughout the polymer matrix is essential to optimize the incorporation of the impermeable clay mineral fillers. As seen with the TEM micrographs, the *in situ* preparation led to a greater dispersion of the layered silicates within the polymer matrix, particularly with 1–5 mass % clay mineral loadings. By improving the clay mineral dispersion, the tortuous diffusion path of the permeating water vapor molecules may be significantly increased, leading to lower WVP results of the *in situ* method over the sonication preparation technique.

### Mechanical Properties

CPN viscoelastic properties, as determined by DMA, were greatly influenced by the differing clay mineral dispersion techniques. The *in situ* technique resulted in increased storage moduli with increased clay mineral loading, while the mixing and sonication dispersion method showed decreased mechanical properties with higher clay mineral content. The DMA storage modulus plots are shown in Figure 6, and storage moduli and cross-link density data is compiled in Table II. CPN preparation from the *in situ* technique led to increased storage moduli up to 5 mass % clay mineral loading. The control coating containing no clay mineral filler recorded a storage modulus at room temperature of 370 MPa. By introducing 1 mass % clay mineral into the polymer matrix, the storage modulus of NCR1_insitu increased to 425 MPa. Further increasing the clay mineral loading to 2 and 5 mass % produced even higher storage moduli, where NCR2_insitu and NCR5_insitu had values of 460 and 510 MPa, respectively. Once the clay mineral loading reached 10 mass %, dramatic reductions in the storage moduli were observed as NCR10_insitu had a storage modulus 100 MPa lower than the control coating at 270 MPa. Increased cross-link density was observed when the clay mineral loading was increased to 2 mass % clay mineral (0.023 mol/cm$^3$), but higher clay mineral content (5–10 mass %) resulted in cross-link densities lower than the control coating (0.016–0.019 mol/cm$^3$). From these results, the peak mechanical performance of the CPNs prepared through the *in situ* process falls with clay mineral loading between 2–5 mass %.

The mixing and sonication clay mineral dispersion route produced CPN films with diminishing mechanical properties as the clay mineral loading is increased, a trend similar to the barrier properties observed by WVT testing. NCR1_sonic measured a storage modulus of 535 MPa at room temperature, but each increment in higher clay mineral content results in a reduction in the storage modulus. When the clay mineral loading reached 10 mass %, the storage modulus of NCR10_sonic was 420 MPa, over 100 MPa lower than NCR1_sonic. The same trend was observed with the crosslink density data, where NCR1_sonic had the highest cross-link density, of the mixing and sonication dispersion technique, at 0.037 mol/cm$^3$, and NCR10_sonic had the lowest value (0.016 mol/cm$^3$). Similar trends in the mechanical performance were observed with the previous study, where increased clay mineral content led to decreased storage moduli and cross-link densities. To better understand this peculiar

**Table III.** Water Vapor Transmission and Permeability

| Sample name | Mass loss/ time (g/h) | WVT (g/m$^2$/s) | Thickness ($\mu$m) | WVP (g·m/m$^2$·s·Pa) |
|---|---|---|---|---|
| Control | 2.15 E-02 | 5.97E-03 | 86 | 8.79E-10 |
| NCR1_insitu | 2.30E-03 | 6.39E-04 | 84 | 9.18E-11 |
| NCR2_insitu | 2.40E-03 | 6.67E-04 | 78 | 8.90E-11 |
| NCR5_insitu | 7.00E-04 | 1.94E-04 | 89 | 2.96E-11 |
| NCR10_insitu | 1.50E-03 | 4.17E-04 | 94 | 6.70E-11 |
| NCR1_sonic | 2.70E-03 | 7.50E-04 | 80 | 1.03E-10 |
| NCR2_sonic | 4.20E-03 | 1.17E-03 | 88 | 1.76E-10 |
| NCR5_sonic | 4.80E-03 | 1.33E-03 | 90 | 2.05E-10 |
| NCR10_sonic | 5.80E-03 | 1.61E-03 | 87 | 2.40E-10 |

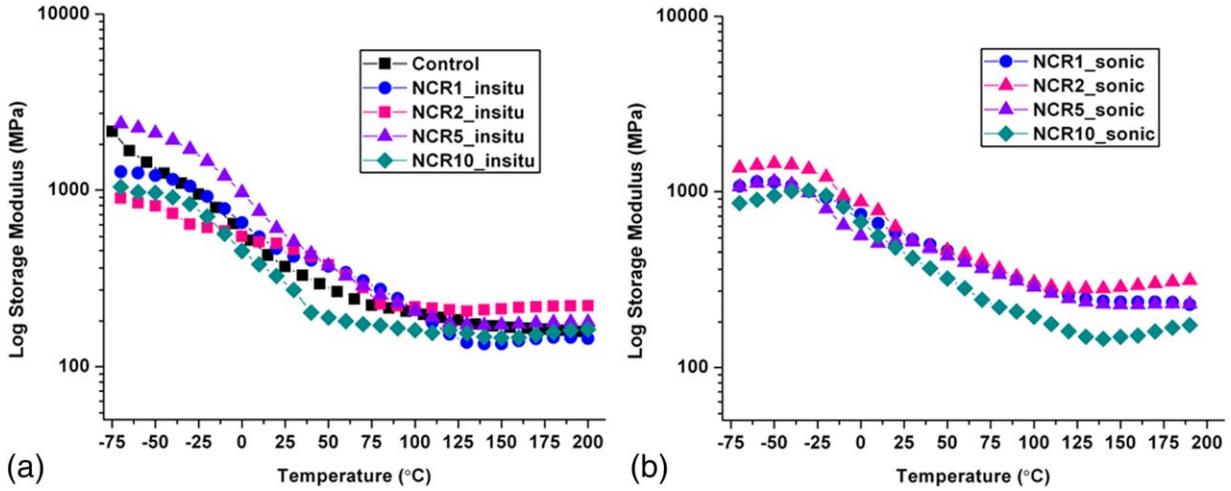


**Figure 6.** DMA storage modulus plots for clay–polymer nanocomposites prepared by the (a) *in situ* technique and (b) mixing and sonication dispersion route. [Color figure can be viewed in the online issue, which is available at wileyonlinelibrary.com.]

behavior, the impact of the organic modifier structure and concentration on the polymer and coating properties was studied.[34] It was determined that the organic modifier, particularly the Cloisite® 30B organic modifier, may plasticize the polymer matrix at high concentrations, leading to reductions in mechanical performance. Based on the mechanical performance of the CPNs in this study, it appears a similar phenomenon may have occurred. In addition to plasticization from the organic modifier, the degree of clay mineral dispersion, particularly the uniformity, may be impacting the final film properties. Because the *in situ* method led to a higher degree of clay mineral dispersion than the mixing and sonication method, the clay mineral fillers of the CPNs prepared through the *in situ* method may be reinforcing the polymer matrix, and thus improving the mechanical properties. Conversely, the sonication preparation method, producing primarily intercalated morphologies with some phase-separation, may not improve the mechanical properties as much due to poorer clay mineral dispersion.

### Thermal Stability and Optical Clarity

Large increases in thermal stability were recorded by the formation of CPNs with clay mineral incorporation through both the *in situ* and mixing/sonication dispersion techniques. The TGA degradation curves shown in Figure 7 and the temperature at 10% mass loss ($T_{10}$%) in Table II display the dramatic improvements in thermal stability with CPN formation. Both dispersion techniques increased the $T_{10}$% values. The control coating recorded a $T_{10}$% of 240°C, whereas for the CPNs, this value increased to 300°C with NCR1_insitu, NCR2_insitu, and NCR1_sonic. The thermal stability declined slightly as the clay mineral loading increased, but the CPN films maintained $T_{10}$% values at least 30°C higher than the control film. CPNs with higher clay mineral loading had somewhat diminished thermal stability compared to CPNs with 1–2 mass % clay mineral loading. Once again, the impact of the clay mineral volume fraction drastically influences the CPN material properties.

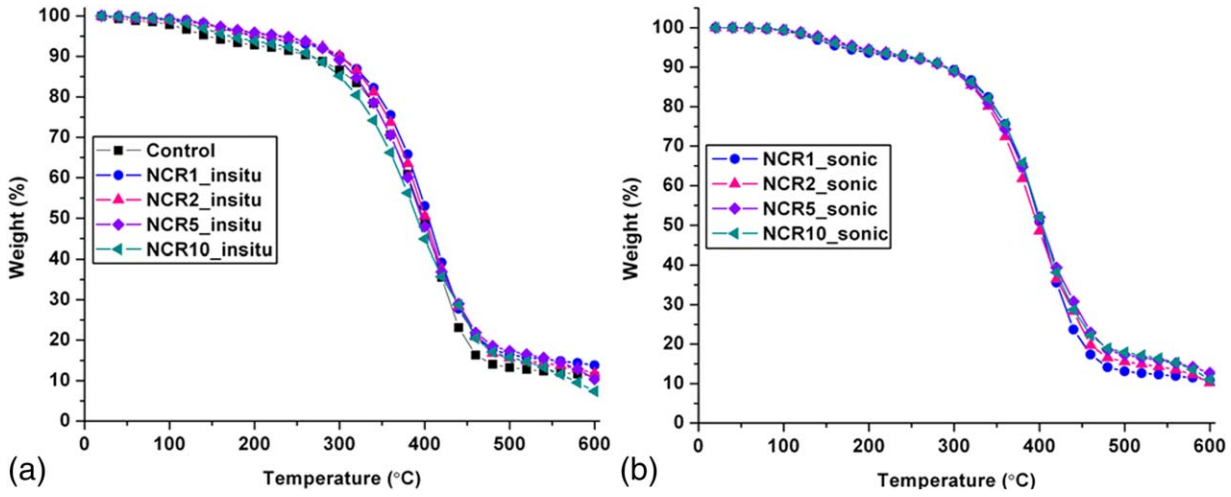


**Figure 7.** TGA plots for clay–polymer nanocomposites prepared by the (a) *in situ* technique and (b) mixing and sonication dispersion route. [Color figure can be viewed in the online issue, which is available at wileyonlinelibrary.com.]

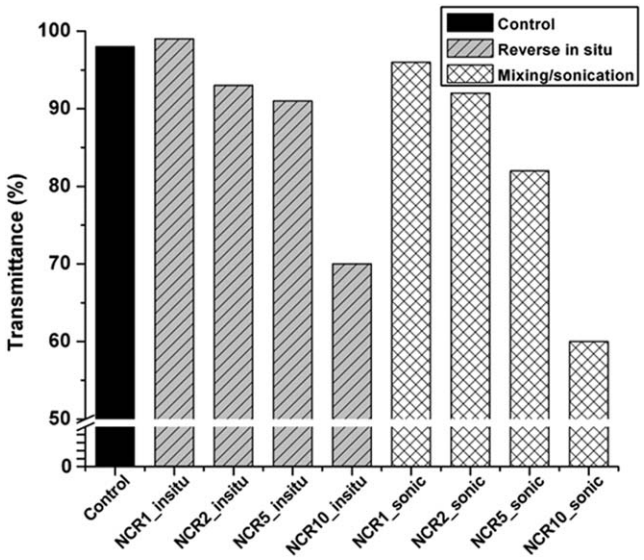


**Figure 8.** Optical clarity of clay–polymer nanocomposite films as determined by percent transmittance at 400 nm from UV–vis spectroscopy.

Two main trends were observed when examining CPN optical clarity: increased clay mineral loading decreased transmittance and the *in situ* technique had higher transmittance values than the mixing and sonication dispersion route for equivalent clay mineral content. Figure 8 displays the reductions in transmittance at higher clay mineral loading, and Table III reports the percent transmittance at 400 nm as determined by UV–vis spectroscopy. CPNs prepared from the *in situ* process maintained high levels of optical clarity (91–99%) with up to 5 mass % clay mineral loading. High transmittance values through these films represent a high degree of uniform clay mineral dispersion throughout the polymer matrix. However, once 10 mass % clay mineral was incorporated into the polymer matrix, the transmittance decreased dramatically to 70% for NCR10_insitu which indicates reductions in homogenous clay mineral dispersion. CPN preparation through the mixing and sonication dispersion route maintained high optical clarity (92–96%) up to 2 mass % clay mineral loading, but higher clay mineral content (5–10 mass %) reduced film transmittance. NCR10_sonic had the lowest transmittance of any CPN prepared in this study at 60%. Since the *in situ* process had higher transmittance values than the sonication dispersion technique for equivalent clay mineral loading, the clarity of these CPNs indicated the *in situ* process produced CPNs with better clay mineral dispersion.

## CONCLUSIONS

Enhanced cure, barrier, mechanical, and thermal properties were observed with the formation of CPNs through a novel *in situ* intercalative synthesis technique. In the polyesters, higher clay mineral volume fractions increased resin viscosity and $M_w$ while decreasing the $T_g$. In the UV-cured films, the *in situ* synthesis technique improved properties, such as increasing conversion up to 15% and decreasing both WVT and WVP. The optimal clay mineral loading was determined to be between 2 and 5 mass % to obtain peak mechanical performance and highest thermal stability. The *in situ* process generated CPNs with significantly better barrier performance, attributed to much better clay mineral dispersion than the sonication preparation route.

## ACKNOWLEDGMENTS

The authors gratefully acknowledge Margaret Piranian for performing the XRD scans, Scott Payne for his help in obtaining TEM micrographs, and The National Science Foundation (EPS-0814442) for funding through North Dakota EPSCoR

## REFERENCES

1. Gilman, J. W. *Appl. Clay Sci.* **1999**, *15*, 31.
2. Leszczyńska, A.; Njuguna, J.; Pielichowski, K.; Banerjee, J. R. *Thermochim. Acta* **2007**, *453*, 75.
3. Pramoda, K. P.; Liu, T.; Liu, Z.; He, C.; Sue, H.-*J. Polym. Degrad. Stab.* **2003**, *81*, 47.
4. Leszczyńska, A.; Njuguna, J.; Pielichowski, K.; Banerjee, J. R. *Thermochim. Acta* **2007**, *454*, 1.
5. Lan, T.; Pinnavaia, T. *J. Chem. Mat.* **1994**, *6*, 2216.
6. Lee, S.-R.; Park, H.-M.; Lim, H.; Kang, T.; Li, X.; Cho, W.-J.; Ha, C.-S. *Polymer* **2002**, *43*, 2495.
7. Zhao, C.; Qin, H.; Gong, F.; Feng, M.; Zhang, S.; Yang, M. *Polym. Degrad. Stab.* **2005**, *87*, 183.
8. Cui, L.; Tarte, N. H.; Woo, S. I. *Macromolecules* **2008**, *41*, 4268.
9. Yeh, J.-M.; Liou, S.-J.; Lai, C.-Y.; Wu, P.-C.; Tsai, T.-Y. *Chem. Mat.* **2001**, *13*, 1131.
10. Gorrasi, G.; Tortora, M.; Vittoria, V.; Pollet, E.; Lepoittevin, B.; Alexandre, M.; Dubois, P. *Polymer* **2003**, *44*, 2271.
11. Kim, J.-K.; Hu, C.; Woo, R. S. C.; Sham, M.-L. *Compos. Sci. Technol.* **2005**, *65*, 805.
12. Herrera-Alonso, J. M.; Marand, E.; Little, J. C.; Cox, S. S. *J. Membr. Sci.* **2009**, *337*, 208.
13. Hsiue, G. H.; Liu, Y. L.; Liao, H. H. *J. Polym. Sci. Part A: Polym. Chem.* **2001**, *39*, 986.
14. Hu, Y.; Wang, S.; Ling, Z.; Zhuang, Y.; Chen, Z.; Fan, W. *Macromol. Mater. Eng.* **2003**, *288*, 272.
15. Bharadwaj, R. K.; Mehrabi, A. R.; Hamilton, C.; Trujillo, C.; Murga, M.; Fan, R.; Chavira, A.; Thompson, A. K. *Polymer* **2002**, *43*, 3699.
16. Galimberti, M.; Cipolletti, V. R.; Coombs, M. *Dev. Clay Sci.* **2013**, *5*, 539.
17. Bergaya, F.; Detellier, C.; Lambert, J. F.; Lagaly, G. *Dev. Clay Sci.* **2013**, *5*, 655.
18. Lambert, J. F.; Bergaya, F. *Dev. Clay Sci.* **2013**, *5*, 679.
19. Rehab, A.; Salahuddin, N. *Mater. Sci. Eng.: A* **2005**, *399*, 368.
20. Sinha Ray, S.; Okamoto, M. *Prog. Polym. Sci.* **2003**, *28*, 1539.
21. Fornes, T. D.; Hunter, D. L.; Paul, D. R. *Macromolecules* **2004**, *37*, 1793.
22. Ke, Y.; Long, C.; Qi, Z. *J. Appl. Polym. Sci.* **1999**, *71*, 1139.

23. Koo, C. M.; Kim, M. J.; Choi, M. H.; Kim, S. O.; Chung, I. J. *J. Appl. Polym. Sci.* **2003**, *88*, 1526.
24. Dennis, H. R.; Hunter, D. L.; Chang, D.; Kim, S.; White, J. L.; Cho, J. W.; Paul, D. R. *Polymer* **2001**, *42*, 9513.
25. Urbanczyk, L.; Ngoundjo, F.; Alexandre, M.; Jérôme, C.; Detrembleur, C.; Calberg, C. *Eur. Polym. J.* **2009**, *45*, 643.
26. Messersmith, P. B.; Giannelis, E. P. *Chem. Mat.* **1993**, *5*, 1064.
27. Paul, M.-A.; Delcourt, C.; Alexandre, M.; Degée, P.; Monteverde, F.; Rulmont, A.; Dubois, P. *Macromol. Chem. Phys.* **2005**, *206*, 484.
28. Tasdelen, M. A.; Van Camp, W.; Goethals, E.; Dubois, P.; Du Prez, F.; Yagci, Y. *Macromolecules* **2008**, *41*, 6035.
29. Kim, D. S.; Kim, J.-T.; Woo, W. B. *J. Appl. Polym. Sci.* **2005**, *96*, 1641.
30. Choi, M. Y.; Anandhan, S.; Youk, J. H.; Baik, D. H.; Seo, S. W.; Lee, H. S. *J. Appl. Polym. Sci.* **2006**, *102*, 3048.
31. Rivero, G.; Vázquez, A.; Manfredi, L. B. *J. Appl. Polym. Sci.* **2009**, *114*, 32.
32. Nikolaidis, A. K.; Achilias, D. S.; Karayannidis, G. P. *Ind. Eng. Chem. Res.* **2010**, *50*, 571.
33. Pavlacky, E.; Ravindran, N.; Webster, D. C. *J. Appl. Polym. Sci.* **2012**, *125*, 3836.
34. Pavlacky, E.; Webster, D. C. *J. Appl. Polym. Sci.* **2013**, *129*, 324.
35. Hill, L. W. *Prog. Org. Coat.* **1997**, *31*, 235.
36. Carothers, W. H.; Arvin, J. A. *J. Am. Chem. Soc.* **1929**, *51*, 2560.
37. Morgan, A. B.; Gilman, J. W. *J. Appl. Polym. Sci.* **2003**, *87*, 1329.